EUROPEAN COMMISSION

Community Research

SEVENTH FRAMEWORK PROGRAMME

CARBOWASTE

Treatment and Disposal of Irradiated Graphite and Other Carbonaceous Waste

Grant Agreement Number: FP7-211333

Deliverable D-4.3.10

Decontamination by Means of LASER Ablation

Author:

M. Lombaard, Necsa, RSA

Document Number: CARBOWASTE-1203-D-4.4.1-a
Date of issue of this report: 09.03.2012

Start date of project: **01/04/2008** Duration : **60 Months**

Project co-funded by the European Commission under the Seventh Framework Programme (2007 to 2011) of the European Atomic Energy Community (EURATOM) for nuclear research and		
Dissemination Level		
PU	Public	
RE	Restricted to the partners of the CARBOWASTE project	
CO	Confidential, only for specific distribution list defined on this document	**X**

This document is the property of NECSA and shall not be used, reproduced, transmitted or disclosed without prior written permission

Distribution list

Person and organisation name and/or group	Comments
WP4 members	
Executive Board	
Co-ordinator	

CARBOWASTE		
Work package: 4 **Task: :** 4.3	**CARBOWASTE document no:** CARBOWASTE-1203-D-4.3.10-a (e.g. May 2008 as date of issue: 0805)	**Document type:** T=Technical Report
Issued by: Necsa, RSA **Internal no.:** CW1203-Deliverable-4-3-10-a		**Document status:** Final

Document title

Decontamination By Means Of Laser Ablation

Executive summary

It is possible and very efficient to use Necsa's Nd:YAG laser system to ablate or decontaminate graphite material. It was shown that the use of a fiber optic cable in conjunction with a focussing lens will enable the laser to cut or drill through the graphite material by only adjusting the focus of the beam (by means of the focussing lens) in accordance to the depth at which the graphite material is ablated. It was also shown that the addition of an automated X, Y, Z translation stage would allow the precise decontamination of large surfaces or foreign objects. This should conclude that the laser system used in this study is a feasible and efficient decontamination tool on contaminated graphite surfaces and can be employed in hostile or inaccessible areas.

Revisions

Rev.	Date	Short description	Author	Internal Review	Task Leader	WP Leader
00	dd/mm/yyyy	Issue	Name, Organisation	Name, Organisation *Signature*	Name, Organisation *Signature*	Name, Organisation *Signature*
01	06/02/2012	First issue	M. Lombaard Necsa	W. Meyer, Necsa		
	09/03/2012	Final issue	M. Lombaard Necsa	W. Meyer, Necsa	D.Vulpius FZJ	von Lensa FZJ

PROJECT REPORT

Carbowaste

DECONTAMINATION BY MEANS OF LASER ABLATION

DOC No: NWR-CAWGEN-REP-12001

Revision: 00

Author: M Lombaard

February 2012

TABLE OF CONTENTS

1 Executive Summary 6

2 Introduction 6

2.1 Background 6
2.2 Aim of the project 8

3 Experimental work 9

3.1 Necsa Nd:YAG laser system 9
3.2 Necsa Nd:YAG laser system with fiber optics 10
3.3 NLC Deckel Maho Nd:YAG laser system 12

4 Results 13

4.1 Determination of laser ablation parameters 13
4.2 Laser ablation without fiber optics 14
4.3 Laser ablation with fiber optics 18
4.4 Laser ablation with Deckel Maho 23

5 Conclusion 24

1 Executive Summary

Laser ablation as a surface decontamination technique was researched as part of the international CARBOWASTE project. A Q-switched Nd:YAG laser system was employed for graphite ablation processes as this type of technology was previously demonstrated at Necsa for the decontamination of metal surfaces. The relationship between ablation rate and laser fluence was investigated after optimal processing conditions were determined. The study was divided into two sections of which the first had an experimental setup that did not include any fiber optic apparatus, while the second employed a fiber optic cable. The latter was to emphasize the versatility of a laser ablation system in areas that pose an occupational hazard towards human beings. Results indicated that both setups could be used as an effective decontamination tool for graphite material at a burst frequency of 10 Hz. Optimal ablation rates for the first and second experimental setup were 1.7×10^{-6} cm^3/J and 5.7×10^{-6} cm^3/J, respectively.

2 Introduction

2.1 Background

Due to the worldwide increase in the use of nuclear power, it is inevitable that a corresponding increase in the number of radioactively polluted facilities and material will occur. The serious challenge of finding suitable storage- or decontamination solutions for hazardous material in order to reduce the threat posed to human beings and the natural environment is a crucial step in nuclear waste management. A number of effective cleaning methods are being investigated in the CARBOWASTE program that include laser ablation cleaning, plasma, acid leaching, and particle blasting.

Laser cleaning is a relatively recent technique for removing pollutants from surfaces but is gaining popularity fast due to its advantages over other techniques. It is known that when laser intensity is high enough, especially in the case of high-power short-pulsed lasers, laser energy absorption occurs rapidly and only in a very thin layer on the target surface. This thin layer is thus instantaneously evaporated and removed without the use

of any cleaning agents. Savina et al[1] described that often the radioactive contaminants in concrete occupied only the surface and near-surface (~3-6 mm deep) regions of the material. As a result, it makes environmental and economic sense to try to remove and store only the thin contaminated layer rather than to treat the entire structure as nuclear waste. This means that laser ablation is considered one of the most effective techniques to clean the radioactively polluted walls of nuclear power plant facilities and other large objects.

The merits of a laser decontamination technique are firstly a remote application, since the laser beam can be delivered remotely via articulated mirrors or fiber optic cables while the ablation head can be manipulated by robots, thus avoiding exposion of workers and the laser system to possible radiation and/or contamination hazards. Secondly, laser ablation only produces a small waste stream that can be easily handled by a scrubber or filter system, due to the fact that no cleaning agents such as detergents are needed. Laser ablation also has a high decontamination factor which makes it a very effective decontamination tool and can be a practical option to recover polluted products under complicated circumstances.

Savina et al also revealed that fragmentation and disaggregation made up the ablation mechanism on the removal of concrete by means of a pulsed Nd:YAG laser ablation system. They found that ablation efficiency was insensitive to peak laser irradiance over the range from 0.2-4.4 MW/cm^2 and that excessive pulse overlap caused a decrease in ablation efficiency due to melting of the material.

Zhou et al[2] performed a study on the surface decontamination of a 20 µm Zn coating on a carbon steel surface by means of a pulsed Nd:YAG laser system. Their investigation included the relationship between ablation rate to laser pulse width and ablation rate to laser fluence, which was used to determine the optimal processing conditions. The behaviour of laser-induced products, which consisted of vapour and liquid particles, was

[1] Savina, M., Xu, Z., Wang, Y., Reed, C., Pellin, M., *Efficiency of concrete removal with a pulsed Nd:YAG laser*, Journal of Laser Applications, Vol. 12, nr. 5, 2000.
[2] Zhou, X., Imasaki, H., Furukawa, H., Yamanaka, C., Nakai, S., *Experimental study on surface decontamination by laser ablation*, Journal of Laser Applications, Vol. 14, nr. 1, 2002.

also studied and it was found that the moving direction of the products was strongly dependant on the incident laser angle. They found that by reducing the incident laser angle, the focussing lens could be protected from the pollutants of the ablated products.

Roberts and Modise[3] investigated the removal of uranyl nitrate and uranium dioxide as a combination of loose and fixed surface contamination from a stainless steel surface by means of a pulsed Nd:YAG laser system. It was found that the loosely bound contamination could be removed from the surface at a laser fluence less than 0.5 J/cm^2. They also showed UO_2 that the ratio of beta to alpha activity was a function of particle size in which larger particles could be removed easier.

Baigalmaa et al[4] also used a Q-switched Nd:YAG laser system to study the decontamination characteristics of Type 304 stainless steel artificially contaminated with surrogate Cs^+ ions. The results showed that more than 98% of the Cs^+ ions were removed after 100 shots at a pulse energy of 450 mJ/pulse and 14 ns pulse width.

These studies prove that laser ablation is a very effective decontamination tool and can be used on various surfaces. In addition, these laser systems can easily be combined with emission spectrometers such as Laser induced breakdown spectroscopy (LIBS) to provide real-time analysis.

2.2 Aim of the project

The aim of this project is to identify if laser ablation could be utilized as a decontamination tool for cleaning contaminated graphite surfaces at Necsa and internationally. The project can be divided into two closely related sections of which the first is normal laser ablation without the use of any fiber optics, while the last section is remote laser ablation with the use of fiber optics. The first section will investigate and confirm some of the ablation parameters on the graphite surfaces, while the second

[3] Roberts, D.E., Modise, T.S., *Laser removal of loose uranium compound contamination from metal surfaces*, Applied Surface Science, Vol. 253, p. 5258-5267, 2007.
[4] Baigalmaa, B., Won, H.J., Moon, J.K., Jung, C.H., Hyun, J.H., *A comprehensive study on the laser decontamination of surfaces contaminated with Cs^+ ion*, Applied Radiation and Isotopes, Vol. 67, p. 1526-1529, 2009.

section will focus more on the versatility of the laser ablation system. This is mainly areas not accessible or suited for humans.

3 Experimental work

3.1 Necsa Nd:YAG laser system

The laser system used for the experiments at Necsa is a U.S. Laser Corporation (Model 406Q) Q-switched Nd:YAG laser. The Q-switch, which is an optical device utilizing Bragg diffraction to spoil the gain of the laser cavity, allowing loss modulation or "Q-switching", allows the laser to operate in a pulse train mode. The laser has four Q-control modes namely Internal Q, Gated Q, Triggered Q, and Gated CW (constant wave). The electronic control unit is used to vary the frequency from single pulse to 50 kHz.

The experimental setup that was used for this study is illustrated in Figure 1.

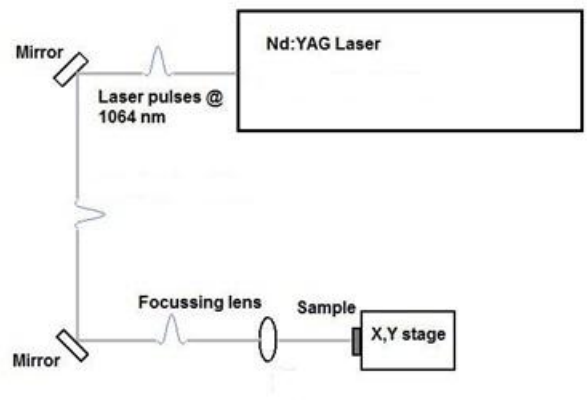

Figure 1. Experimental setup of Nd:YAG laser ablation system at Necsa.

A laser beam with a wavelength of 1064 nm, pulse duration of 67 – 220 nm (depending on the frequency), burst frequency of 0.01 – 50 kHz, and waist diameter of 4.1 mm, was produced at a lamp current of 35 Amperes. The laser beam was then focussed onto the target surface by a plano-convex lens with a focal length of 55 mm. The incident angle was set at 90°.

For the laser setup discussed above (Section 3.1) and the next with the fiber optic cable attached (Section 3.2), the focussed beam was used to ablate graphite material at a specific point on a fixed graphite sample. This allowed the beam to drill a ditch into the graphite material, which could be analysed to determine the ablation parameters.

3.2 Necsa Nd:YAG laser system with fiber optics

For the fiber optic work, the experimental setup was similar to the one illustrated in Figure 1 except that the beam was delivered by a fiber optic cable instead of the conventional mirrors. The beam delivery system used in this study included the input coupler, gradient index fiber and the output coupler. The input coupler together with its mount assembly was responsible for positioning the fiber and focusing the laser beam into the fiber. An appropriate multi-element lens, was used to focus the laser beam to a spot diameter small enough to fully couple the beam into the fiber core, which in this study was 800 µm. The lens was mounted in a three axis adjustable mount, which provided X /Y adjustment of the fiber, and a Z axis lens focus. Figure 2 shows the input coupler for the used laser system.

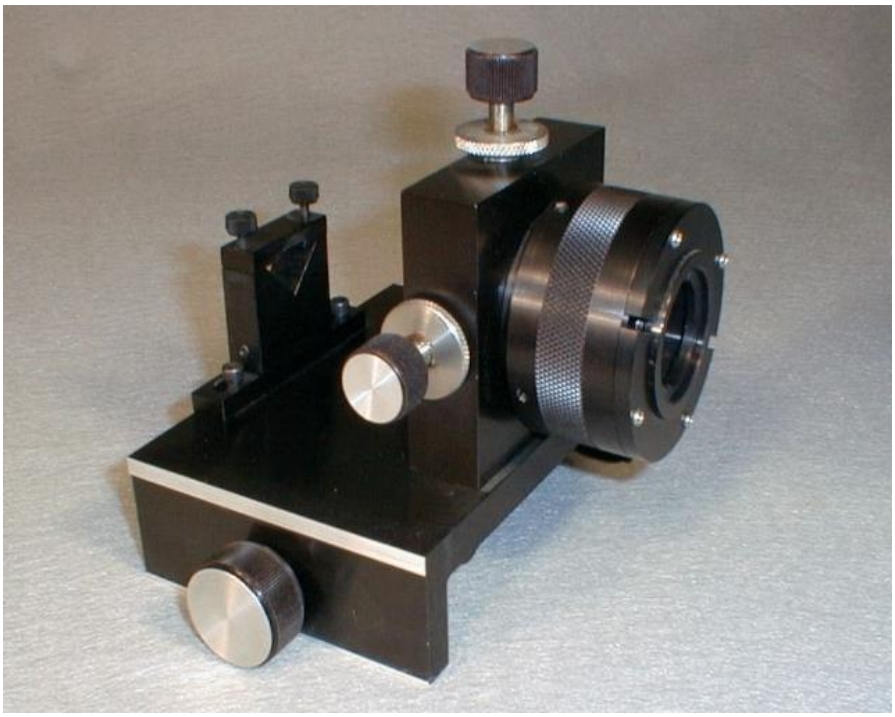

Figure 2. Input coupler for U.S Laser Corp Nd:YAG laser system.

The gradient index fiber optic cable, which had a doped fused silica core, had a core diameter starting at 1000 µm to 500 µm. Thus, the beam was focused inside the fiber optic cable in the same way a normal lens focuses a beam. The fiber is effectively lossless, except for approximately 8% Fresnel loss at the end faces.

The output coupler is a multi-element assembly which first collimates the diverging beam from the fiber output (the output collimator section), and then re-focuses it to form an image of the fiber core (the output objective assembly). A connector on the collimator assembly is provided for easy attachment of the fiber. The lenses are mounted in precision machined in-line housings, and are pre-aligned to the fiber. Figure 3 shows the output collimator assembly used for this laser system.

Figure 3. Output collimator for U.S Laser Corp Nd:YAG laser system.

The ablated ditch was measured with a FEI Quanta 200 3D (Scanning Electron Microscope) to determine the area, from which the ablated volume was calculated.

3.3 NLC Deckel Maho Nd:YAG laser system

For decontamination of surfaces, it is necessary to implement some form of an automated translation stage either onto the laser head or the sample. This would enable the user to program the translation stage for a specific area where decontamination is required. The program then ensures that the laser beam is guided to the required location to perform the ablation activities.

To illustrate the effectiveness of such an automated system, the Deckel Maho Nd:YAG laser system at the National Laser Centre (NLC) was employed. The laser system has an automated X, Y, Z translation stage that can handle samples of up to 50 kg. The table has a maximum scan speed of 800 mm/s with a focus point (distance of focus lens from sample) of 100 mm. The operation wavelength is the standard 1064 nm with a pulse width of 250 ns and changeable frequency range of 5-50 kHz. The spot size of the focussed beam is 40 µm.

For this experiment, the translation stage was programmed to ablate a 1 cm^2 square on the graphite sample at a scan rate of 80 mm/s. The scan procedure was such that the direction of ablation was from left to right for each row and from top to bottom (like reading a book). This was to ensure that even ablation could be maintained for the duration of the scan by eliminating any hot spots caused by overlapping pulses. See Figure 4 to compare the correct method with the incorrect method.

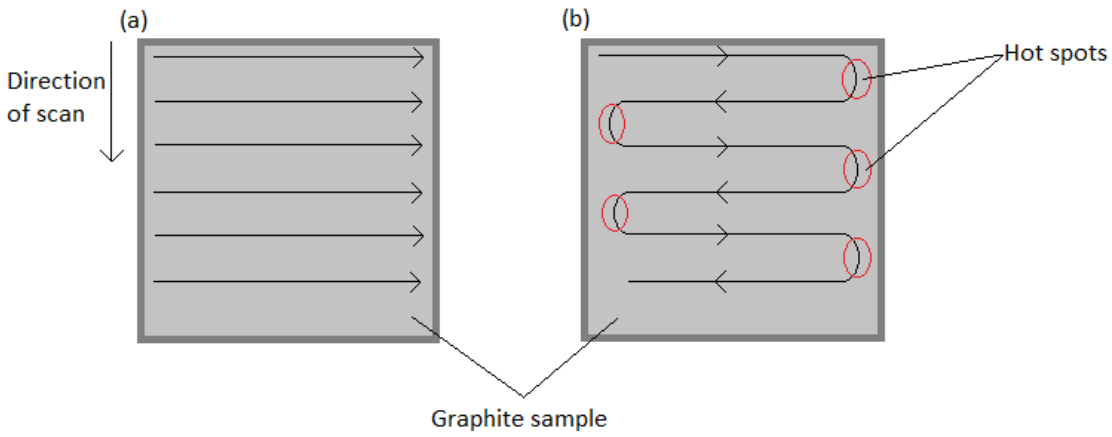

Figure 4(a) Correct scan method and (b) incorrect method that generates hot spots at the sides of the scan area.

4 Results

4.1 Determination of laser ablation parameters

The first experiment performed was the measurement of laser power generated over the 0.01 – 50 kHz frequency range (Figure 4). This was done to determine what frequency corresponded to the maximum power output for this laser system. The Q-switch was set to internal-mode, which meant that the controller directly Q-switched the laser at the rate set on the digital panel meter.

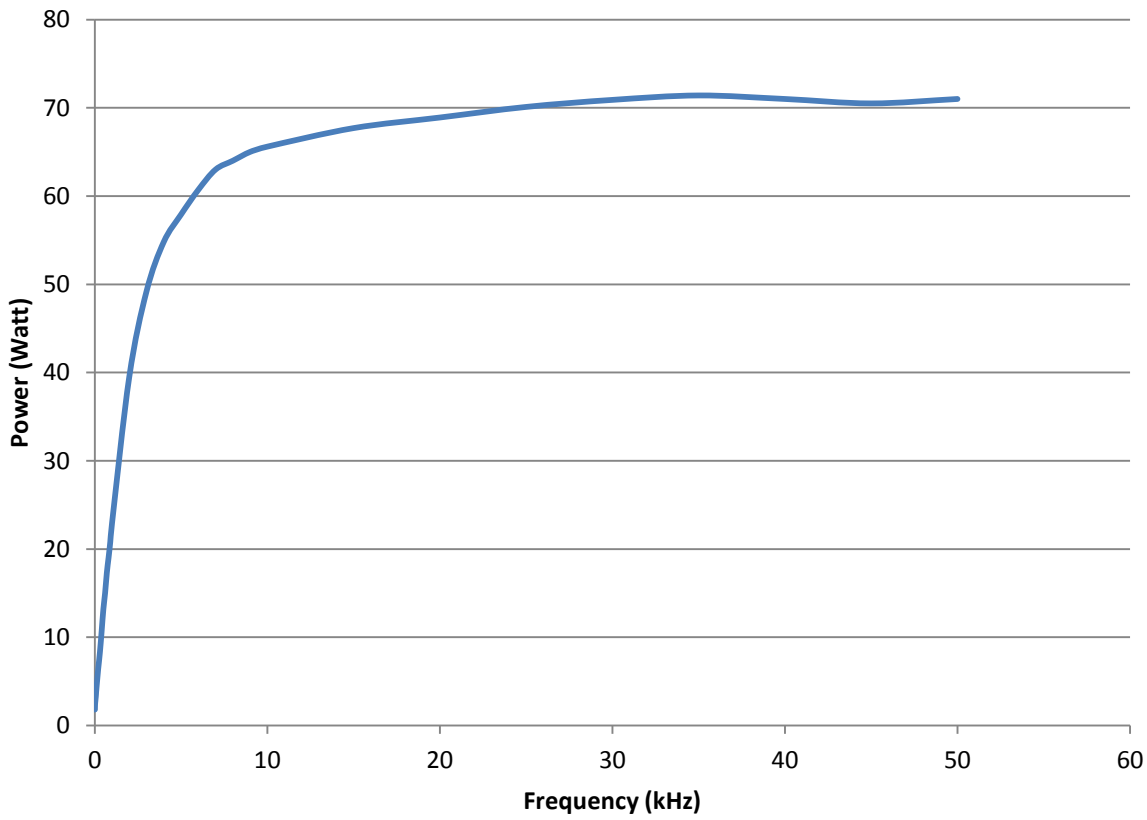

Figure 5: Average power in Watts versus the Q-switch frequency in kHz.

The results in Figure 5 suggested that the average power increased as the frequency increased, reaching a maximum average power of 71.4 W at 35 kHz. This suggested that the increase in pulses as the frequency was increased caused the overall power to increase up to 35 kHz. However, as the laser system comes closer to reaching its maximum frequency output the power starts to slowly decrease again. The pulse energy over the frequency range could then be determined as follows:

$$E = \frac{P_{Av}}{R_{Rate}} \quad (1)$$

Where: E = Energy in Joules

P_{Av} = Average power in Watts

R_{Rate} = Repitition rate in pulses per second

The calculated pulse energy against frequency is given in Figure 6.

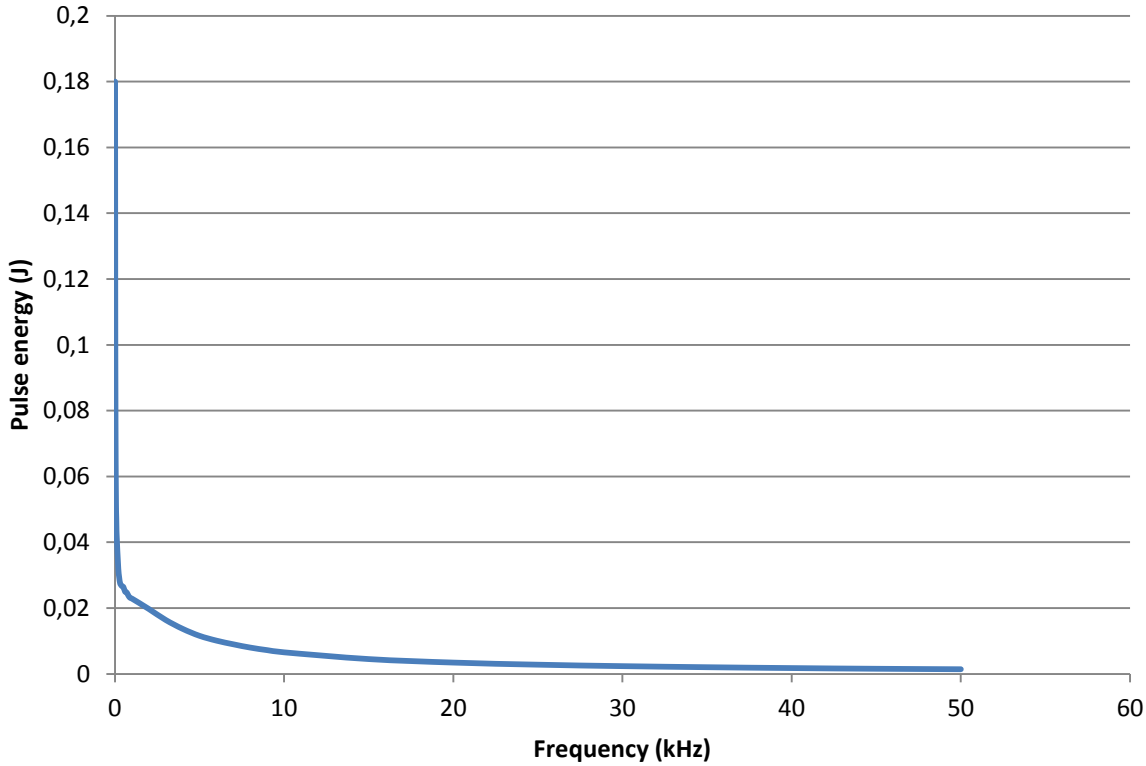

Figure 6: Pulse energy in Joule versus frequency in kHz.

The results in Figure 6 suggested that the energy per pulse decreased dramatically as the frequency increased reaching a maximum pulse energy of 0.18 J at 0.01 kHz and minimum of 0.00142 J at 50 kHz.

4.2 Laser ablation without fiber optics

By using the plano-convex focussing lens, the beam was focussed to a spot size with a radius of 0.0221 cm and area of 0.00153 cm^2. The focussing of the beam helped to concentrate the energy from the laser, which on its own would not achieve ablation, to achieve an energy density high enough for ablation. It should be noted that the pulse energy will stay constant at a certain frequency but the fluence (energy density) can be

varied by just changing the spot size. The fluence/energy density (Figure 7) was then calculated at the different frequencies by means of equation 2.

$$F = \frac{E_p}{A} \quad (2)$$

Where: F = Fluence in J/cm^2

E_p = Pulse energy in Joules

A = Area of spot in cm^2

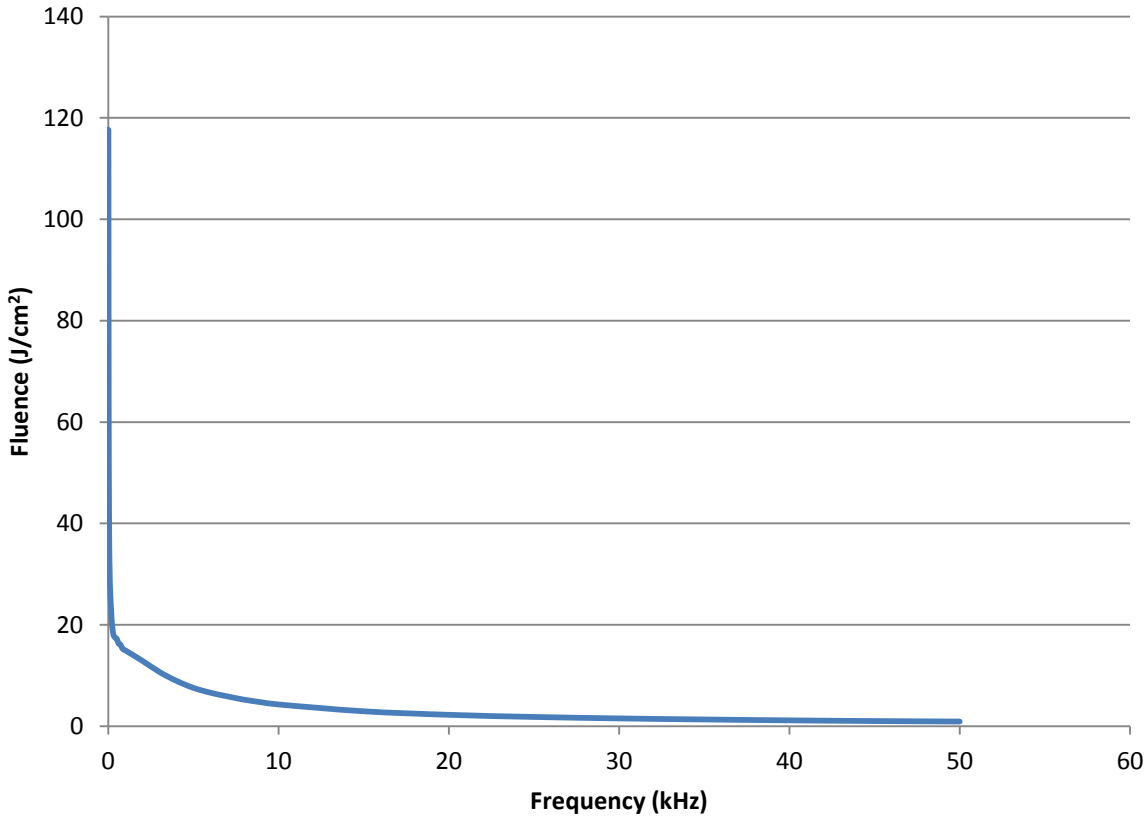

Figure 7: Calculated fluence of Nd:YAG laser at different frequencies.

The results suggested that the highest fluence of 117.647 J/cm^2 was measured at 10 Hz, which corresponded to the highest pulse energy. This allowed for much higher pulse energies at the cost of a reduced number of pulses per second. The lowest fluence was observed at 50 kHz. The effect of these parameters on the ablation efficiency/ablation rate onto graphite can be seen in Figures 8, 9, 10 and 11.

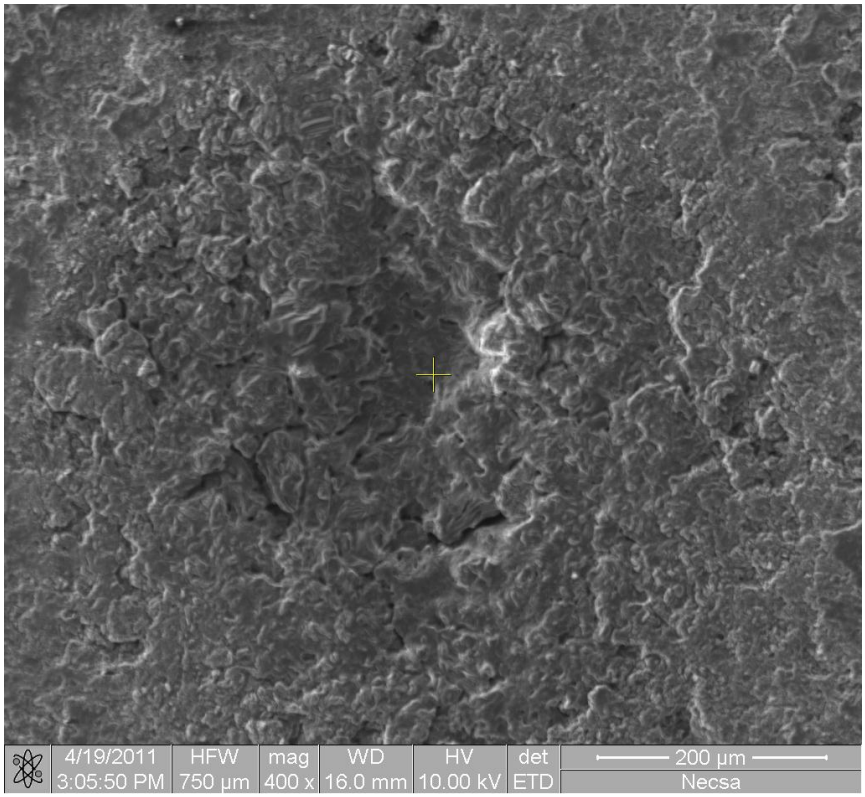

Figure 8: Ablation of graphite sample with focussed Nd:YAG laser at 1 kHz for 10 seconds.

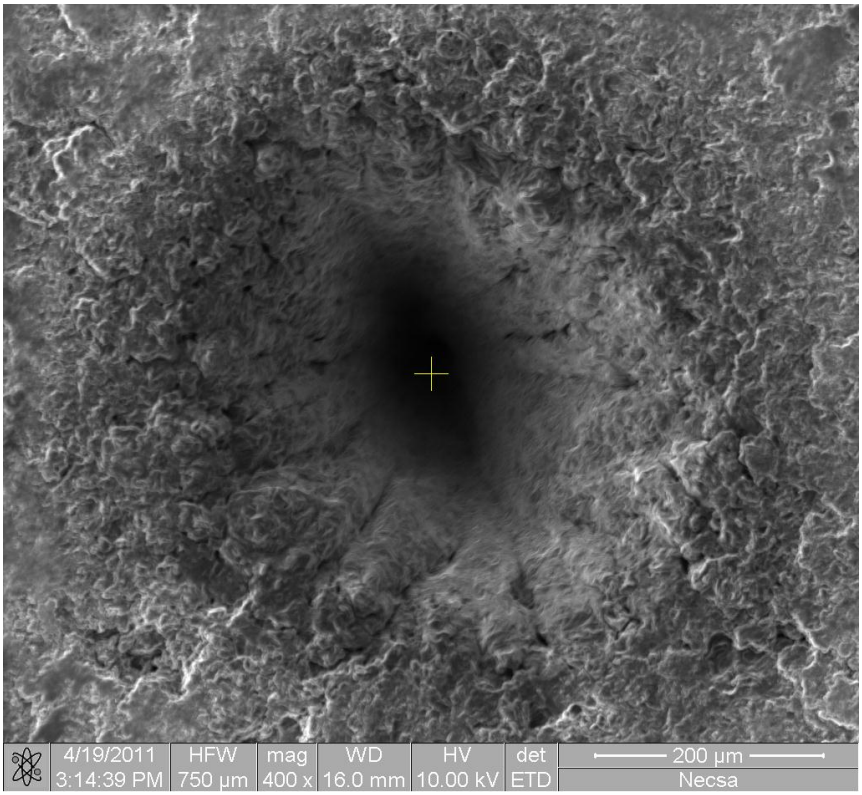

Figure 9: Ablation of graphite sample with focussed Nd:YAG laser at 10 Hz for 10 seconds.

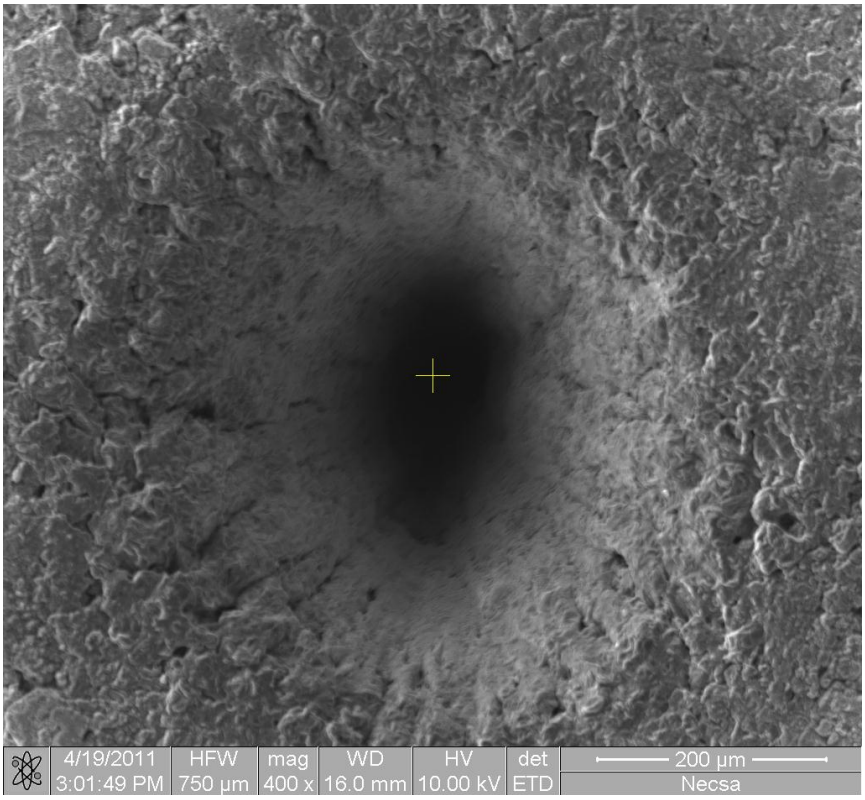

Figure 10: Ablation of graphite sample with focussed Nd:YAG laser at 1 kHz for 1 min.

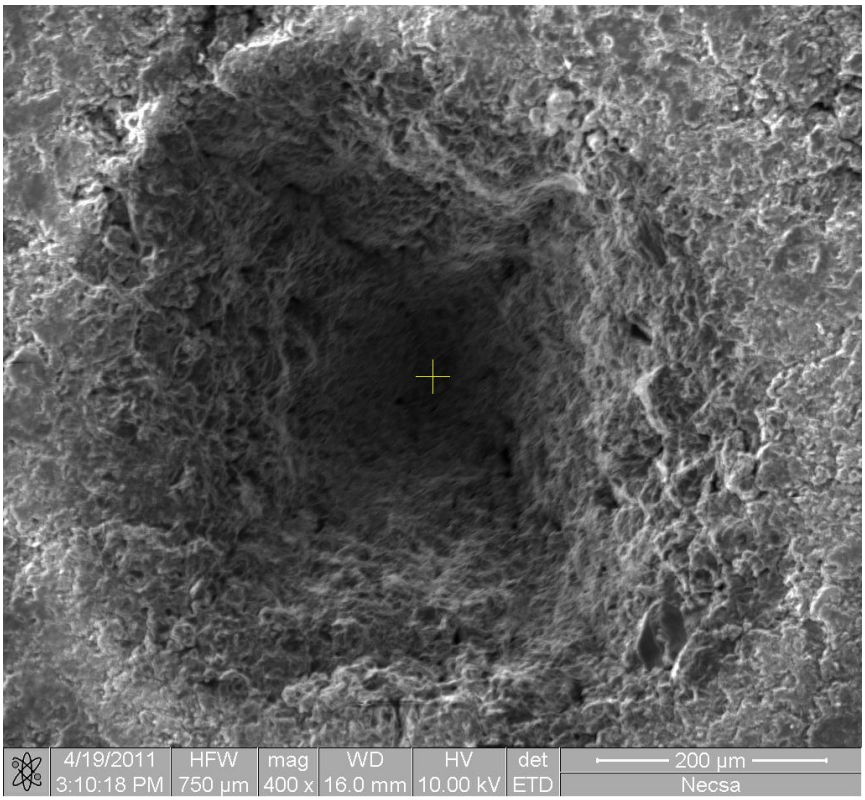

Figure 11: Ablation of graphite sample with focussed Nd:YAG laser at 10 kHz for 1 minute.

The ablation rate is defined as ablated volume divided by consumed laser energy:

$$R_a = \frac{V}{E} \quad (3)$$

where R_a is the ablation rate, V is the ablation volume and E is the laser energy. This is used to express the material removal ability of laser ablation. Thus, at higher ablation rates, more material can be removed with less laser energy.

The ablation rate at 10 Hz, 1 kHz and 10 kHz was calculated to be 1.7×10^{-6} cm^3/J, 2.8×10^{-8} cm^3/J and 8×10^{-9} cm^3/J, respectively. This suggested that at 10 Hz the laser was able to ablate 60 times more efficient than at 1 kHz and 200 times more than 10 kHz.

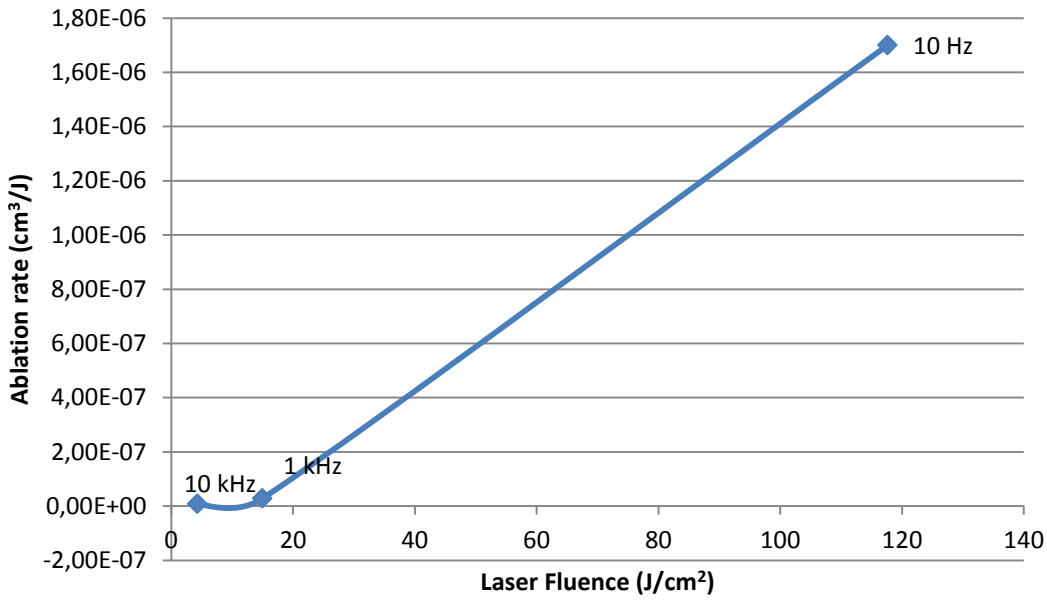

Figure 12. Ablation rate at various laser fluencies for Nd:YAG laser system without fiber optic cable.

4.3 Laser ablation with fiber optics

As explained in the Experimental Section the use of the fiber optic cable and output coupler did not only provide a medium in which the beam could be transported to the sample but also allowed the beam to be focused onto the sample. This ensured that the beam had a perfectly round profile and allowed a much higher energy density (fluence)

due to the fiber's profile. After exiting the fiber and passing through the focussing lens, the beam diameter varied between 402 – 470 µm, depending on how far the sample was from the lens. This variation in beam diameter also resulted in different energy densities which could be plotted against the ablation rate to determine where the best ablation rate is.

Figure 13 shows the graphite sample after it was ablated at 10 Hz for the duration of 10 seconds. At this frequency and ablation time the total number of pulses was 100. It was the lowest frequency (except for single shot) and highest pulse energy that could be achieved with this laser.

The fluence at 10 Hz was calculated at 141.73 J/cm^2 for an area of 1.27 × 10^{-3} cm^2. The area was calculated for a spot diameter of 402.54 µm. The depth of the ablated ditch (hole) was 805 µm, which gave a ditch volume of 1.02 × 10^{-4} cm^3.

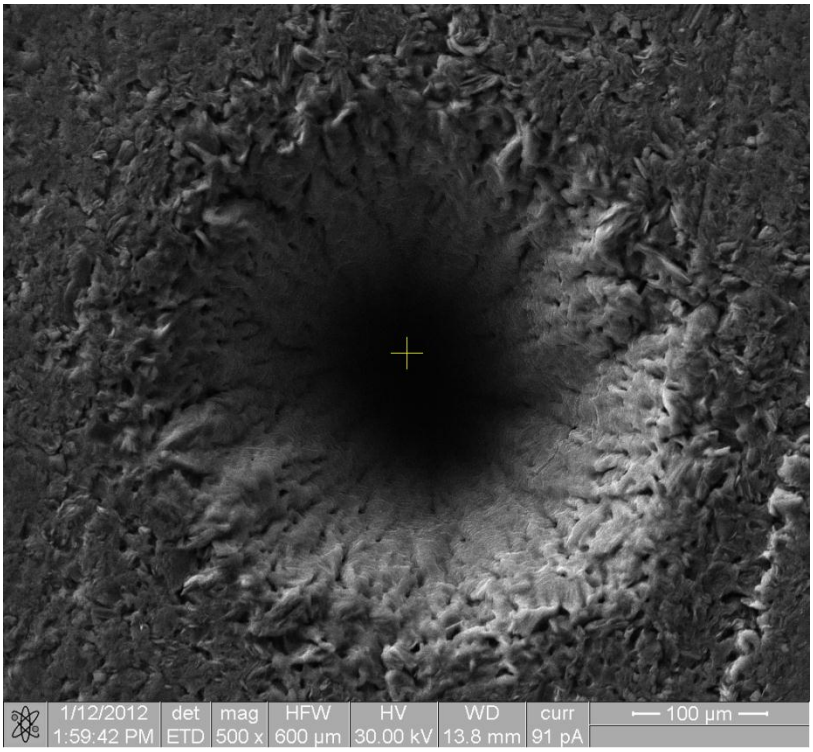

Figure 13. SEM photo of the graphite sample after laser ablation at 10 Hz for 10 seconds using a fiber optic cable.

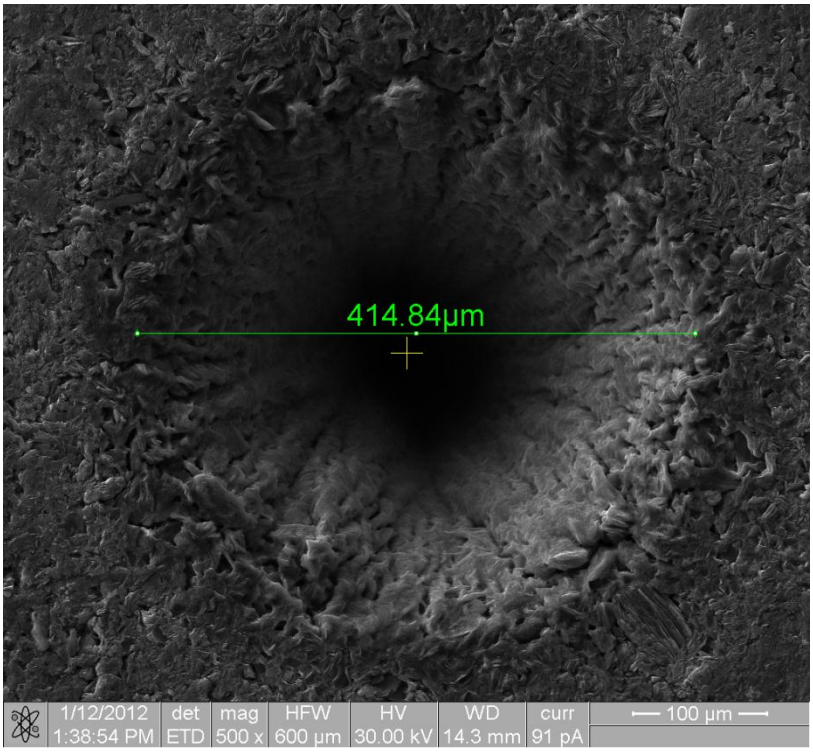

Figure 14. SEM photo of the graphite sample after laser ablation at 100 Hz for 10 seconds using a fiber optic cable.

Figure 14 shows a SEM photo of the graphite sample after it was ablated at 100 Hz for the duration of 10 seconds. At this frequency and ablation time the total number of pulses was 1000. The fluence at 100 Hz was calculated at 31.48 J/cm^2 for an area of 1.35×10^{-3} cm^2. The area was calculated for a spot diameter of 414.84 µm. The depth of the ablated hole was 800 µm, which gave a ditch volume of 1.08×10^{-4} cm^3.

Figure 15 shows the graphite sample after it was ablated at 1 kHz for the duration of 10 seconds. At this frequency and ablation time the total number of pulses was 10000. The fluence at 1 kHz was calculated at 13.17 J/cm^2 for an area of 1.74×10^{-3} cm^2. The area was calculated for a spot diameter of 470.51 µm. The depth of the ablated hole was 564 µm, which gave a ditch volume of 0.981×10^{-4} cm^3.

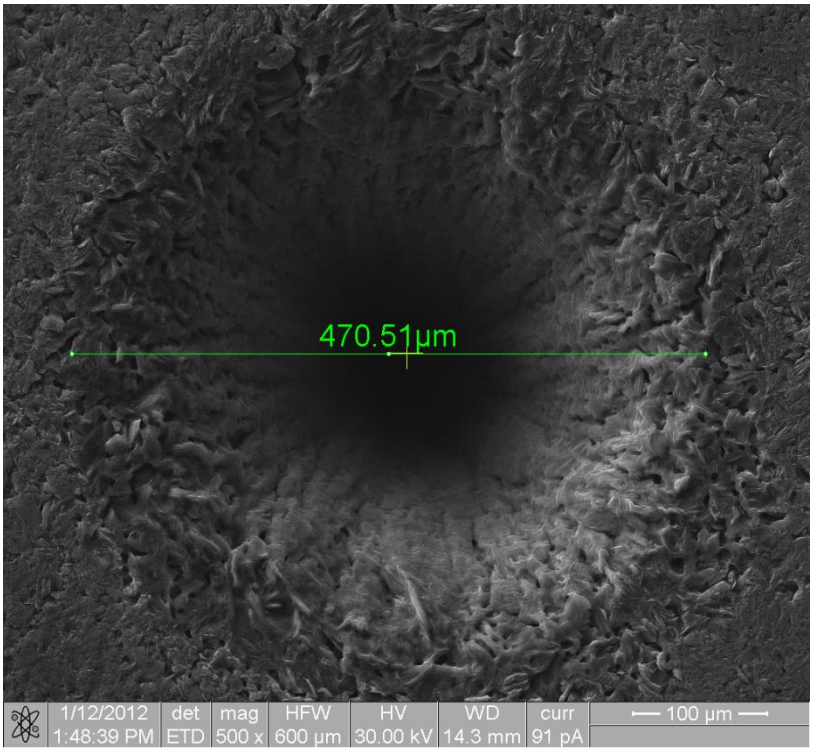

Figure 15. SEM photo of the graphite sample after laser ablation at 1 kHz for 10 seconds using a fiber optic cable.

Figure 16 shows the graphite sample after it was ablated at 10 kHz for the duration of 10 seconds. At this frequency and ablation time the total number of pulses was 100000. The fluence at 10 kHz was calculated at 4.30 J/cm^2 for an area of 1.525 × 10^{-3} cm^2. The area was calculated for a spot diameter of 440.63 µm. The depth of the ablated hole was 200 µm, which gave a ditch volume of 0.305 × 10^{-4} cm^3. At this frequency much of the energy exerted on the sample were lost to heating of the sample. It was observed that the entire surface of sample had a temperature increase of about 20 °C for this short duration. As a result, it is expected that this frequency will not produce high ablation rates since any heat dissipation throughout the sample will strongly influence (negatively) the ablation efficiency.

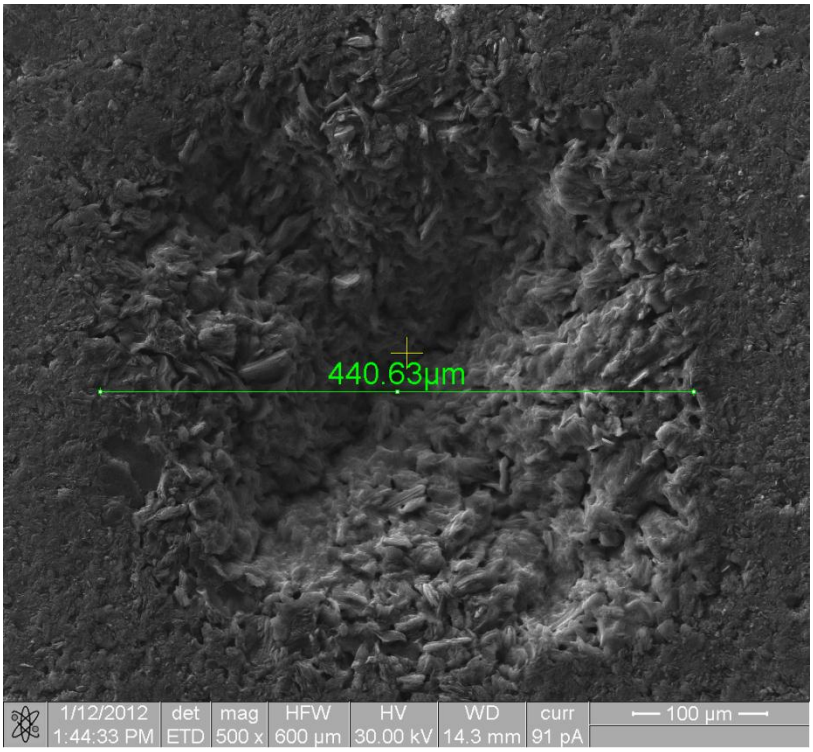

Figure 16. SEM photo of the graphite sample after laser ablation at 10 kHz for 10 seconds using a fiber optic cable.

By using equation 3 the rate of material removability could be determined. Table 1 shows a summary of the ablation parameters at the various frequencies for the work performed with the fiber optic system.

Table 1: Ablation parameters for fiber optic laser system

Frequency	Pulse Energy (J)	Fluence (J/cm^2)	Ablated Volume (cm^3)	Ablation rate (cm^3/J)
10 Hz	0.18	141.73	1.02×10^{-4}	5.7×10^{-6}
100 Hz	0.043	31.48	1.08×10^{-4}	2.5×10^{-6}
1 kHz	0.0229	13.17	9.81×10^{-5}	4.3×10^{-7}
10 kHz	0.00656	4.30	3.05×10^{-5}	4.6×10^{-8}

Figure 17 shows the relationship between ablation rate and laser fluence for this experiment. The results suggested that at 100 Hz the laser was able to ablate a larger volume of graphite in the 10 seconds compared to any other frequency. However, at this frequency a total of 43 Watt was needed to create the ablated ditch. In contrast, at

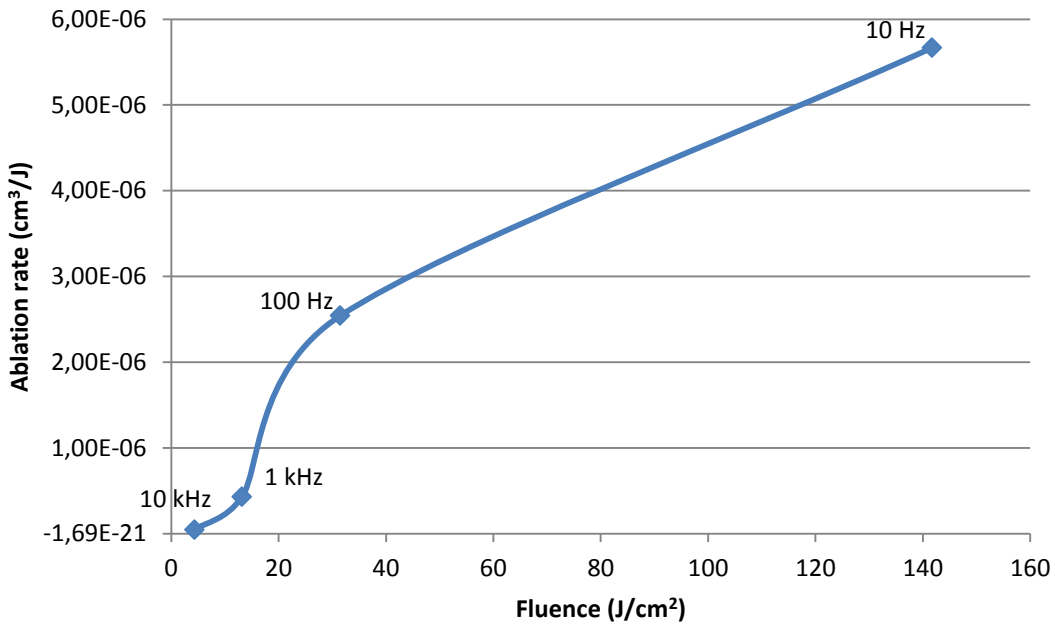

Figure 17. Ablation rate at various laser fluencies for Nd:YAG laser system with fiber optic cable.

10 Hz the total laser power needed to create a slightly smaller (difference of 6×10^{-6} cm^3) ditch was only 18 Watt. This meant that at 10 Hz, less than half of the laser power at 100 Hz was needed to create a ditch that was only slightly smaller. As a result, the ablation efficiency at 10 Hz was higher than at 100 Hz.

As expected at 10 kHz, the ablation rate was very poor due to heat generation and should therefore not be considered as a frequency to do ablation work with this fiber optic system on the graphite material.

4.4 Laser ablation with Deckel Maho

To illustrate the benefit of using an automated X, Y, Z translation stage, the NLC's Deckel Maho was employed. This laser system provided the means to precisely and accurately ablate a predefined area on the graphite sample at chosen ablation parameters. Figure 18 shows the graphite sample after a 1 cm^2 area was ablated at a frequency of 40 kHz, pulse duration of 200 ns and scan rate of 800 mm/s.

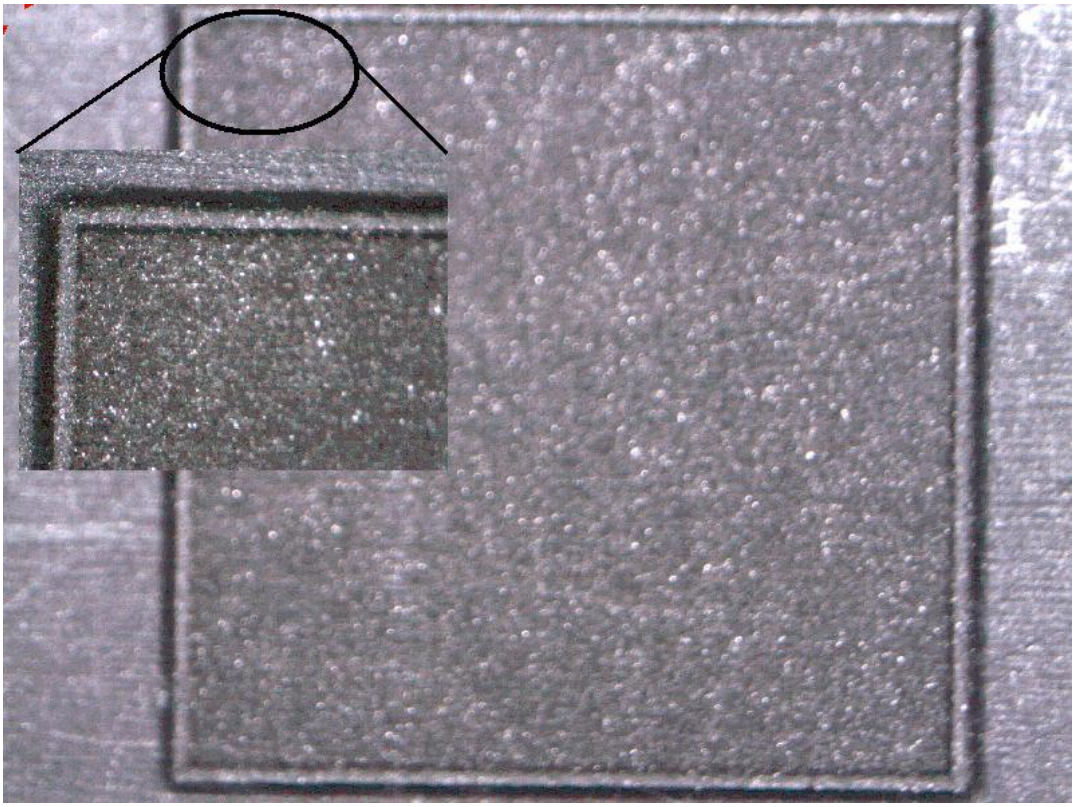

Figure 18. Ablated area of the graphite sample after it was irradiated with the Deckel Maho Nd:YAG laser system.

The volume of the ablated area was measured to be 2×10^{-4} cm^3 (1 cm in length and width, and 2 µm in depth). The laser system was able to ablate 1 µm in depth of the graphite material during each pass of the focussed beam. The translation stage was programmed to account for the graphite material as it was ablated and correspondingly adjust the beam focus in order to ensure that the same focus was maintained during each scan cycle. The figure clearly illustrates how precise the automated X, Y, Z translation stage can manoeuvre the sample for accurate ablation.

5 Conclusion

As demonstrated in Section 4.3, it is possible and very efficient to use Necsa's Nd:YAG laser system to ablate or decontaminate graphite material. It was shown that the use of a fiber optic cable in conjunction with a focussing lens will enable the laser to cut or drill through the graphite material by only adjusting the focus of the beam (by means of the focussing lens) in accordance to the depth at which the graphite material is ablated. It

was also shown that the addition of an automated X, Y, Z translation stage would allow the precise decontamination of large surfaces or foreign objects. This should conclude that the laser system used in this study is a feasible and efficient decontamination tool on contaminated graphite surfaces and can be employed in hostile or inaccessible areas.